ARTICLES

LO−TO Splittings in Plasma-Deposited Siloxane Films

B. Cláudio Trasferetti[†] and Celso U. Davanzo*

Instituto de Química, Universidade Estadual de Campinas, Caixa Postal 6154, CEP-13.083-862, Campinas -SP, Brazil

Mário A. Bica de Moraes

Instituto de Física "Gleb Wataghin", Universidade Estadual de Campinas, Caixa Postal 6165, CEP-13.087-970, Campinas -SP, Brazil

Received: December 11, 2002; In Final Form: June 27, 2003

The present work presents LO and TO functions in the mid-infrared region for thin films deposited from glow discharge plasmas of tetramethylsilane (TMS) diluted either in Ar or O_2 or in mixtures of these two gases. These functions were calculated through the Kramers−Krönig analysis of transmittance spectra of the films supported on KBr disks. To correlate structural aspects of the films with the observed LO−TO splittings, a group frequency analysis based on the literature was made. Such an analysis indicated that the films deposited from the TMS−Ar mixture were formed mainly by a polycarbosilane skeleton, whereas those deposited from TMS−O_2 and TMS−O_2−Ar were formed by a random network of four types of distorted tetrahedra: $(CH_3)_3SiO_{0.5}$, $(CH_3)_2SiO$, $(CH_3SiO_{1.5})$, and SiO_2. From the LO−TO splitting for the asymmetrical stretching mode of Si−O−Si groups, the density and the presence of defects in samples obtained from TMS−O_2 and TMS−O_2−Ar mixtures were evaluated. The number of defects increased as the Ar-to-O_2 flow rate decreased. We also report for the first time LO−TO splittings for bands related to the bending of CH_3 and to the stretching of the Si−C bond in $Si(CH_3)_x$ groups. The knowledge of such splittings is very important for a correct evaluation of the infrared reflection−absorption spectra taken at oblique incidence of thin films containing Si−O bonds and $Si(CH_3)_x$ groups deposited on metals.

I. Introduction

Owing to their unique chemical and surface properties, polymer films deposited from organosilicon and oxygen mixtures by plasma-enhanced chemical vapor deposition (PECVD) find numerous applications. Usually they combine favorable characteristics, such as high-temperature endurance and insulating qualities of conventional polyorganosiloxanes with the advantageous features of plasma-deposited polymeric coatings. These features include a dense, amorphous, cross-linked and pinhole-free structure, high thickness uniformity, and excellent adhesion to metal and insulator substrates. They are becoming increasingly important in many aspects of device technology, such as intermetal dielectric applications,[1−6] and in the packaging industry to deposit oxygen barriers on polymers. Depositions of films from oxygen-free organosilicon monomers are also very interesting from the technological point of view as they can give rise to the formation of preceramic polycarbosilanes (polymers whose skeleton is formed by Si−CH_2−Si groups) that can generate SiC when pyrolyzed.[7] SiC has been increasingly used in the fabrication of advanced electronic devices and is regarded as an extremely promising semiconductor.[7] Therefore, knowledge of the structure and properties of silicon-containing plasma-polymers is a key to the development of effective materials for all these applications.

Several monomers can be used to generate silicon plasma polymers. Tetramethylsilane (TMS), hexamethyldisiloxane (HMDSO), and tetraethoxysilane (TEOS) are among the ones most used. Cyclosiloxanes, such as hexamethylcyclotrisiloxane, have also been employed recently. However, the possibility of synthesizing oxygen-free materials is a clear advantage of TMS in relation to the siloxane and alkoxysilane monomers.

Infrared (IR) spectroscopy is an important tool for the structural characterization of these materials, because it is rather accessible and provides invaluable chemical information. Traditionally, IR characterization has been made from the analysis of experimental transmittance spectra of the films deposited on transparent materials, acquired at normal incidence. There are even some reports of spectra acquired from samples made of film material scratched from the substrate and mixed with powdered KBr. However, the number of scientific works reporting analysis of longitudinal optical (LO) and transversal optical (TO) frequencies has been increasing, particularly in investigations of v-SiO_2 and v-SiO_2-like structures.[8−19] Because of the intensive investigations on this area, important and detailed information about these materials has been obtained.

* To whom correspondence should be addressed. E-mail: celso@iqm.unicamp.br.

[†] Present address: Instituto de Física "Gleb Wataghin", Universidade Estadual de Campinas, Caixa Postal 6165, CEP-13.087-970, Campinas-SP, Brazil.

10.1021/jp027694d CCC: $25.00
Published on Web 09/10/2003

To our knowledge, however, silicon polymers have not yet been investigated using this approach. The polysiloxane-like structures can have high concentration of Si−O−Si groups and, as in v-SiO_2, can give rise to the observation of LO−TO splittings of Si−O−Si-related bands. Knowledge about LO−TO splittings is important both for a correct interpretation of spectra taken at conditions giving rise to the observation of LO bands, such as reflection−absorption spectra taken at off-normal angles, and for structural information about the material, such as density of defects. The latter issue is related to the fact that LO−TO splittings are a consequence of long-range Coulombic interactions for a given oscillator and are therefore sensitive to any kind of network breaks, such as dangling bonds, network terminations, porosity, and the presence of groups different from that constituting the skeleton (for instance, Si−CH_2−Si groups in a siloxane network).

The purpose of this paper is therefore 2-fold. On one hand, we will report a traditional IR characterization based on detailed band assignments by comparison with the available literature; on the other, we will both present and analyze LO and TO functions for PECVD films deposited from tetramethylsilane (TMS). TMS was chosen because, when mixed with oxygen, it is the simplest organosilicon monomer appropriate for generation of controlled amounts of Si−O−Si groups. This meets our special concern in this paper, which is to assess LO modes in solids having different concentrations of Si−O−Si groups. By profiting from all of the information about SiO_2 structures gathered throughout the past years, we hope to provide a basis for the transfer of knowledge from this area to the field of silicon polymers and to divulge experimental results that could be further investigated by means of theoretical studies. It is also important to remark that we observed LO−TO splittings for other modes, especially those involving Si−C oscillators in $Si(CH_3)_x$ groups, and this is also reported for the first time.

II. Background

Lattice vibrations are often described in terms of the wavevector **K**, whose modulus is $2\pi/\lambda$ and whose direction is that of the propagation of the oscillatory movement of the crystal lattice. Because the wavelength in the infrared is of the order of 10^4 nm and the typical dimension of a unit cell is of the order of 1−10 nm, the radiation only interacts with lattice vibrations that exhibit a long wavelength, i.e., with vibrations for which the modulus of **K** tends to zero.[20,21] In transverse optical (TO) modes, the atomic displacements are perpendicular to the direction of the periodicity of the elastic wave (that of the wavevector **K**), whereas in the longitudinal ones (LO), the displacements are parallel to the wavevector. So, for a single vibration, there exist two types of transitions. When polarizable media is concerned, LO and TO modes are not coincident.[20,21]

Although the LO−TO splitting phenomenon is clear for crystals, for which **K** is a well-defined property, this is not the case with amorphous materials. Although there is some controversy concerning the existence of LO−TO splitting in disordered materials, its occurrence in partially ionic glasses has previously been observed in several glass systems.[9,11,12,17−19,22] Galeener and Lukowsky[22] were the first investigators to observe such splittings in tetrahedral glasses and stressed that, because they are due to long-range Coulombic effects, these forces should be included in complete theories of the vibrational properties of many glasses. Since their observations, several authors have confirmed the occurrence of LO−TO splittings in glassy AX_2 systems by means of theoretical calculations.[15,16,23−25]

Specifically for the case of LO and TO modes in amorphous SiO_2 structrures, several articles have been published.[9,11,15,16] There seems to be a consensus over the assignment of the three detached TO bands in the IR spectrum of v-SiO_2. Each of them is paired with a LO mode and can be characterized in terms of a particular mode of motion of the oxygen atoms with respect to the silicon atom pair which they bridge: (i) the lowest-frequency TO band centered at 450 cm^{-1} is assigned to the rocking (R) motion, (ii) the middle TO band, which is centered at 800 cm^{-1}, is assigned to symmetrical stretching (SS) motion, and (iii) the remaining TO band (1070 cm^{-1}) is due to an asymmetrical stretching (AS) motion.

However, it has been observed that there is a high-frequency shoulder in this last TO band which, according to several investigators, suggests that the AS motion actually gives rise to two vibrational modes:[9] (1) an AS1 mode in which adjacent O atoms execute the AS motion in phase with each other and (2) an AS2 mode in which adjacent O atoms execute the AS motion 180° out of phase with each other. The AS1 mode is characteristic of the vibrational behavior of the TO band centered at 1072 cm^{-1}, whereas the shoulder at ∼1200 cm^{-1} is related to the AS2 mode. According to Kirk,[9] the AS1 mode causes the activation of the IR-inactive AS2 mode through a disorder-induced mechanical coupling mechanism. Sarnthein et al.[15] presented strong evidence through comparisons between neutron scattering data and calculations carried out by first-principles density functional theory that it is really a doublet and cannot be ascribed to a LO−TO effect. Their results were corroborated by our investigations on v-SiO_2 reflectance spectra taken at oblique incidences for both p- and s-polarized light.[19] We showed that the shoulder was still observed even if an alternative Kramers−Krönig analysis using a s-polarized spectrum as the input data was carried out. Because it is widely known that s-polarized light cannot detect LO modes, the shoulder is supposed to have a TO character.

The effects of network reticulation on LO and TO functions have also been explored in two papers. Kamitsos and co-workers[11] investigated sol−gel silica that was subjected to heat treatments, therefore, inducing the formation of structures with variable porosities of the Si−O−Si network. They observed that an increase in the temperature of the heat treatment favored an increase in the LO−TO splitting for all bands. This effect was attributed to the strengthening of the long-range Coulombic interactions due to increasing network cross-linking through formation of Si−O−Si bridges during heating. Another relevant observation made by them is that the high-frequency shoulder in the TO function associated with the AS2 mode intensity was enhanced by low temperature heat treatment. Studying silica structures with different porosities, Guiton and Pantano[12] showed that, with increasing porosity, the maxima of the LO and TO functions were converging toward frequencies intermediate between the LO and TO modes of fused silica. Such behavior was explained by using effective medium theory (EMT) calculations. Both studies are very important as they showed the limitations of the traditional view that changes in the absorption spectra of porous silicas are strictly due to structural features.

LO and TO modes of amorphous SiO_2 systems have also been explored in the characterization of thin films and the SiO_2/Si interface, which is very important from the standpoint of semiconductor device technology.[18,26]

III. Experimental Section

IIIA. Thin Film Deposition. Film depositions were carried out in a stainless steel vacuum chamber fitted with two

TABLE 1: Deposition Parameters, Thicknesses, Refractive Indices and the Deposition Rates of the Investigated Films

sample	F_{Ar} (sccm)	F_{O2} (sccm)	d (nm)	n ($\lambda = 633$ nm)	$\Delta d/\Delta t$ (nm/min)
S1−Al, S1−KBr, and S1−Si	18	0	120	1.67	6
S2−Al, S2−KBr, and S2−Si	12	6	247	1.48	12
S3−Al, S3−KBr, and S3−Si	6	12	375	1.46	19
S4−Al, S4−KBr, and S4−Si	0	18	460	1.46	23

horizontal parallel plate water-cooled electrodes of 11 cm diameter. The upper electrode was connected to a radio frequency generator (40 MHz, 100 W max. power) while the lower one was grounded. The chamber was pumped by a 150 m^3/h Roots pump backed by a 22 m^3/h rotary vane pump. A Pirani manometer was used for pressure readings. High purity argon and oxygen were admitted to the chamber using precision electronic mass flow meters. The source of TMS (Aldrich) vapor, a 60 cm^3 glass bulb containing liquid TMS, was connected to the chamber via a precision leak valve. To keep the temperature of the liquid constant during evaporation, the cell was immersed in a room-temperature water bath. The partial pressure of TMS in the discharge was kept at 6 Pa for all depositions. Table 1 summarizes the deposition parameters, thicknesses, refractive indices, and the deposition rates of the samples discussed in this paper. As substrates, we used (i) aluminum-coated glass substrates for reflection−absorption measurements, (ii) KBr disks for transmission measurements, and (iii) silicon wafers for thickness and refractive index measurements. Film thicknesses were determined using a profilemeter (Veeco-Dektak3), and the refractive indices were measured using the Abèles method employing the 632.8 nm line of a He−Ne laser.[27] The deposition conditions were labeled as S1, S2, S3, and S4 according to an increasing flow rate of oxygen in the discharge. Accordingly, the samples were named after the deposition condition label and the substrate used. For example, S1−Al refers to sample deposited on aluminum using the deposition conditions S1.

IIIB. Infrared Spectra Acquisition. Both the infrared transmission and reflection−absorption spectra were measured for all samples in a Bomen MB-101 FT-IR spectrometer equipped with a DTGS (deuterated triglycine sulfate) detector. The spectral range covered was 400−5000 cm^{-1}. Each spectrum was the result of co-adding 64 scans collected at 4 cm^{-1} resolution, in the transmission and external-specular-reflectance modes. For the reflection−absorption measurements, a variable-angle attachment (SPECAC) was used. The incidence angle was 70° off-normal, and the incident beam was p-polarized. Polarization was provided by the insertion of a grid polarizer (SPECAC) in the optical path. All reflection−absorption measurements were referenced to an aluminum mirror, whereas the transmission ones were referenced to a bare KBr disk. Both types of measurements were carried out at room temperature.

IIIC. Data Analysis. TO and LO energy-loss functions (F_{TO} and F_{LO}, respectively), whose maxima correspond to the TO and LO vibrational modes, respectively, are related to the complex dielectric function $\tilde{\epsilon}$

$$F_{TO} = \mathrm{Im}[\tilde{\epsilon}(\nu)] \tag{1}$$

$$F_{LO} = \mathrm{Im}[-1/\tilde{\epsilon}(\nu)] \tag{2}$$

where ν is the wavenumber in cm^{-1}. For nonmagnetic materials

$$\tilde{\epsilon} = \tilde{n}^2(\nu) = [n(\nu) + ik(\nu)]^2 \tag{3}$$

where $\tilde{n}$ is the complex refractive index, n is the refractive index, and k is the absorption index. Thus, we need the optical constants [$n(\nu)$ and $k(\nu)$] to determine F_{TO} and F_{LO}.

The absorption indices of the films was calculated from the transmittance spectra of the films deposited onto KBr disks by means of the following expressions:

$$A(\nu) = -\log[T(\nu)] \tag{4}$$

$$k(\nu) = \frac{A(\nu)}{4\pi\nu d} \tag{5}$$

where A is the absorbance, T is the transmittance, and d is the film thickness in cm. For the determination of the refractive index n, it should be remembered that, because $\tilde{n}$ is a causal parameter, its real and imaginary parts are related to each other by the so-called Kramers−Krönig transformation (KKT).[28] Therefore n(ν) was calculated by the following equation:[29]

$$n(\nu') = n_\infty + \frac{2}{\pi} p \int_0^\infty \frac{\nu k(\nu')}{(\nu^2 - \nu'^2)} \tag{6}$$

where n_∞ can be taken as the refractive index in the visible range and the symbol p refers to the principal part of the integral. As for the extrapolation required by the above equation, absorption indices obtained from the first and last points of the measured spectrum file were assumed constant.[28]

We propose here a procedure for assessing the quality of the retrieved $\tilde{n}$ by simulating reflection−absorption spectra of a thin film deposited on aluminum and comparing them with experimental ones. The simulation was carried out through the Fresnel equation for a three-phase layered system, which has been described elsewhere.[30]

IV. Results

IVA. Kramers−Krönig Analysis of Transmittance Data. Figure 1, parts a−d, shows an example of the application of the procedure described above to sample S4−KBr. From the transmission spectrum of the film deposited on the KBr disks, the k values were calculated as a function of the wavenumber using eq 4 and 5, and the result is plotted in Figure 1b. Application of the KKT to the k spectrum yields $n(\nu)$ values (Figure 1c). Finally, $n(\nu)$ and $k(\nu)$ were used in the Fresnel equation for a three-layered system[30] to simulate the reflection−absorption spectrum of the sample deposited on aluminum (the optical constants of aluminum, necessary for this calculation, were taken from ref 31), represented by the full line in Figure 1d. Also shown in this figure is the experimental reflection−absorption spectrum of sample S4−Al. The parameters for both the experimental and the simulated spectra are incidence angle of 70° and p-polarized light. The excellent agreement between the simulated and the experimental spectra supports the reliability of the optical constants determination procedure. Although not shown here for the sake of brevity, similar results were obtained for the other samples.

The high transmittivity and the straight and constant baseline observed in all spectra are attributed to the high degree of coherence of the deposited materials.

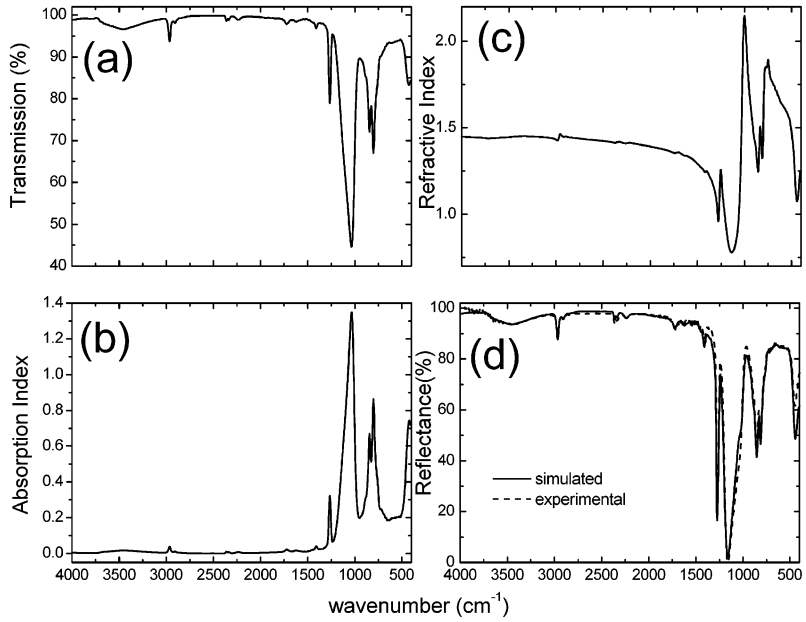

Figure 1. (a) Transmission spectrum of film S4−KBr, (b) absorption index spectrum calculated from transmission spectrum using eq 5, (c) refractive index spectrum calculated from the absorption index spectrum using the Kramers−Krönig transformation, and (d) simulated and experimental reflection−absorption spectra (p-polarized light and incidence angle of 70°) of film S4−Al.

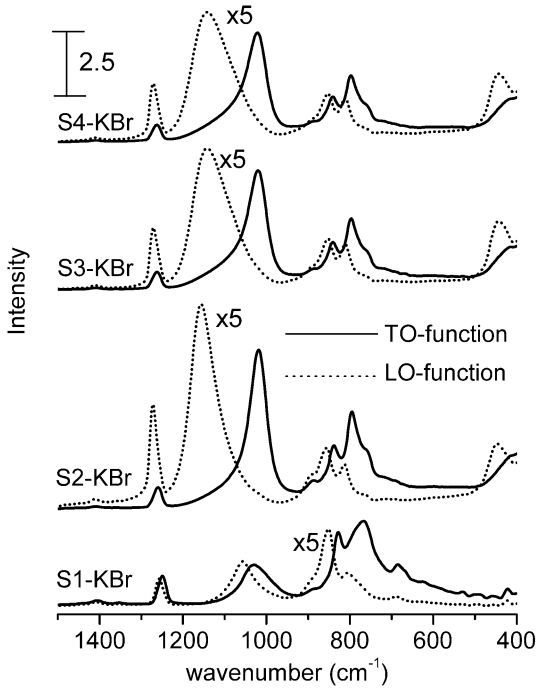

Figure 2. LO and TO functions (low-frequency region) for the samples S1−KBr to S4−KBr calculated according to the procedure outlined in section IIIC. Note that the intensity of the LO functions was multiplied by a factor of 5 to match the TO function intensities.

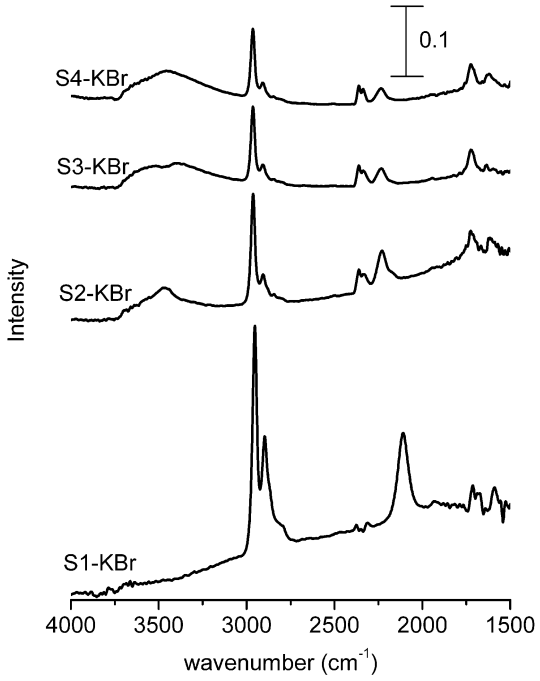

Figure 3. TO functions (high-frequency region) for samples S1−KBr to S4−KBr, calculated by the same procedure as in Figure 2.

IVB. Chemical Groups Forming the Films. Both the LO and TO functions for samples S1−KBr to S4−KBr were calculated by the previously outlined procedure in the 4000−400 cm^{-1} range. Figure 2 exhibits both functions in the low-frequency region (1500−400 cm^{-1}), whereas Figure 3 shows F_{TO} in the high-frequency region (4000−1500 cm^{-1}). Only F_{TO} is shown in Figure 3 because F_{LO} and F_{TO} are practically superimposed in the wavenumber range shown.

From Figures 2 and 3, assignments have been made from the literature[32−38] and are shown in Table 2. Only F_{TO} was considered because all of the literature available on the subject is based on transmission measurements taken at normal incidence, with which only TO modes can be detected. Some of the absorption bands in the spectra of Figures 2 and 3 show the presence of groups that are present (−CH_3 and Si−CH_3) and absent (Si−O−Si and Si−H) in the precursor molecule, which is in agreement with the fragmentation and further fragment recombination taking place during the deposition process. A detailed discussion on all the observed groups is presented below.

(1) Si−O−Si Groups. From Figure 2, the most prominent TO bands for samples S2−KBr, S3−KBr, and S4−KBr, at 1018, 1021, and 1021 cm^{-1}, respectively, are assigned to the Si−O−Si asymmetrical stretching mode. It will be termed AS1 mode, in analogy to v-SiO_2, for which it lies at 1072 cm^{-1}.[19] In the spectrum of v-SiO_2, there is a high-frequency shoulder

TABLE 2: Infrared Band Assignments from the Literature

band maximum (cm^{-1})							
S3−KBr and S4−KBr		S2−KBr		S1−KBr			
TO	LO	TO	LO	TO	LO	assignment[a]	refs
	444		448			ρ_{Si-O} in Si−O−Si	32
				685	689	$\nu_{S,Si-C3}$	33
∼760 (sh)		∼760 (sh.)		768	804	ρ_{Me},ν_{SiC} in Si−Me_3 or Si−Me_1	32
796	810	794	813			ρ_{Me},ν_{SiC} in Si−Me_2	32
841	853	839	856	827	851	ρ_{Me},ν_{SiC} in Si−Me_3	32
1021	1140	1018	1157	1030	1057	$\nu_{AS,SiO}$ in Si−O−Si[b]	32,34
1263	1272	1259	1272	1248	1257	$\delta_{S,Me}$ in Si−Me_x	32
				1354	1354	γ_{CH2} in Si−CH_2-Si	34
1409	1410	1409	1411	1405	1407	$\delta_{AS,Me}$ in Si−Me_x	32
1621	1621					$\nu_{C=O}$	38
1723	1725	1725	1726			$\nu_{C=O}$	38
2235	2235	2231	2233	2110	2113	ν_{Si-H}	32
2906	2906	2905	2906	2896	2898	$\nu_{S,C-H}$ in Si−Me_x	32
2965	2965	2962	2964	2953	2956	$\nu_{AS,C-H}$ in Si−Me_x	32

[a] ν, δ, ρ, γ, and ω denote stretching, bending, rocking, scissoring, and wagging modes, respectively; AS and S denote asymmetric and symmetric vibrations. [b] For film S1−KBR, there is also a contribution of the ω_{CH2} mode in Si−CH_2−Si.

of the AS1 band that is attributed to an asymmetrical stretch (AS2) in which adjacent O atoms execute the motion 180° out of phase with each other. For most of samples of Figure 2, in lieu of this characteristic shoulder, a tail is present which causes the band to be inhomogeneously broadened. Because we are dealing with a system that, apart from the presence of methyl groups, is much like v-SiO_2, it is likely that the high-frequency tails observed are related to the an incipient AS2-like mode of v-SiO_2. For samples S2−KBr, S3−KBr, and S4−KBr, fwhm values for this TO band were 47, 50, and 53 cm^{-1}, respectively. Because LO−TO splitting of the AS2 mode is expected to be both reversed (see ref 9) and less intense than that of the AS1 mode, the LO band envelope should be even more inhomogeneously broadened. The fwhm values observed were 70, 95, and 105 cm^{-1} for films S2−KBr, S3−KBr, and S4−KBr, respectively. Because an increase in the AS1:AS2 intensity ratio has been associated with an increase in defects in SiO_2 structures,[11,12] these fwhm values show that the presence of defects in the film increased as the O_2-to-Ar flow rate increased. These defects comprise the presence of network terminating groups, such as Si−Me_3, porosity, and the presence of groups such as C═O and Si−H. Such relative increases in defect sites may be a consequence of a high concentration of O_2 in the plasma discharge. It has been proposed that exposure of the growing film to oxygen species bombardment during the deposition process can result in the formation of both defects consisting of free radicals and dangling bonds, which are subject to oxidation upon exposure to the atmosphere.[39]

The appearance of the AS1 modes at frequencies lower to that of v-SiO_2 has also been observed for structures bearing a suboxide bonding arrangement, e.g., the SiO_x films deposited by PECVD investigated by Lucovsky and co-workers[40] and Pai and co-workers.[1] Furthermore, Si−O−Si absorption bands within the range 1055−1024 cm^{-1} have been observed for polymeric siloxanes.[40] The fact that samples S2−KBr, S3−KBr, and S4−KBr do not exhibit a clear splitting of the AS1 mode indicates a network rather than a polymeric character.[39,41]

Another distinguishing Si−O feature is the Si−O bond rocking mode. For thermal SiO_2, it is located at 450 cm^{-1}.[9] A red-shift is also expected for SiO_x-like materials. We could not determine precisely the position of the maxima of the TO function of samples S2−KBr, S3−KBr, and S4−KBr, either because of the low sensitivity of the spectrometer detector in this wavenumber region or the possibility that the maxima lie below 400 cm^{-1}. However, for the LO function, the maxima were located at ∼445 cm^{-1}, which lie at a lower wavenumber as compared to the LO maximum observed for thermal SiO_2 (505 cm^{-1}). The absence of this band in both TO and LO-function for sample S1−KBr is noteworthy.

(2) Si−$(CH_3)_x$. The bands at 2955 and 2898 cm^{-1} for S1−KBr and 2965 and 2906 cm^{-1} for the other samples are assigned to methyl groups attached to silicon atoms. For each sample, the band lying at higher frequency is due to the asymmetrical C−H stretching, and the one lying at lower frequency is due to the symmetrical stretching. These assignments agree with two well-known facts relating methyl groups in siloxane and aliphatic compounds: in siloxanes both bands are much weaker and the symmetric stretching lies in a higher frequency region for siloxane compounds.

All four samples exhibit a TO-band located at 1248 and 1259 cm^{-1} for samples S1−KBr and S2−KBr, respectively, and 1263 cm^{-1} for samples S3−KBr and S4−KBr assigned to Si−Me_x groups. For TMS, the band due to this group appears at 1250 cm^{-1}. This band has been studied by a number of investigators and there is no doubt that it is due to symmetric methyl deformation. Although the band is known to be reasonably strong and therefore easily recognized, it increases in frequency when the silicon atom is linked to oxygen.[7] The asymmetrical deformation mode of the methyl group is considered to be of less interest. It occurs as a weak band near 1410 cm^{-1}, and it is thus of very limited use for identification purposes. Although very weak, all four samples exhibited this band at 1410 cm^{-1}.

All four samples exhibit strong absorptions in the 900−600 cm^{-1} range due to normal modes involving coupling of the rocking of methyl groups and stretching of Si−C bonds. Because, analagous to C−H stretchings, methyl rockings are also supposed to be less intense when the carbon atom involved in the movement is linked to silicon, the high intensity of the bands we observed in the 900−600 cm^{-1} range is probably due to the contribution of Si−C stretchings.[37] Three different bands are directly observed: (i) one between 760 and 770 cm^{-1} (observed as shoulders for samples S2−KBr, S3−KBr and S4−KBr), which can be associated to both $SiMe_3$ and $SiMe_1$, (ii) one at ∼795 cm^{-1} (observed as a shoulder for sample S1−KBr) related to $SiMe_2$ groups, and (iii) one between 827 and 841 cm^{-1}, which is also associated with $SiMe_3$ groups. It seems that the latter is very sensitive to oxygen concentration because it blue-shifted as the film was deposited in the presence of oxygen.

The spectra of film S1−KBr also shows the presence of a low-intensity band related to trimethylsylil groups at 685 cm^{-1}. Such a band is also observed in the spectrum of TMS and was assigned to the asymmetrical stretching in SiC_3 groups of organosilicon compounds through theoretical studies made by McKean and co-workers.[37] This band is not observed in the spectra of films deposited in the presence of O_2. Therefore, the film S1−KBr is supposed to have the higher concentration of $SiMe_3$ groups, which is in agreement with the assumption that the presence of O_2 in the discharge increases the degree of fragmentation of the monomer molecule.

(3) Si−CH_2−Si. Owing to the absence of O_2 in the discharge, sample S1−KBr presents characteristics that are different from those of the other films. The TO band observed at 1030 cm^{-1} can also be assigned to the wagging mode (ω) of methylene in Si−CH_2−Si groups,[34] which is the basis of the skeleton of the

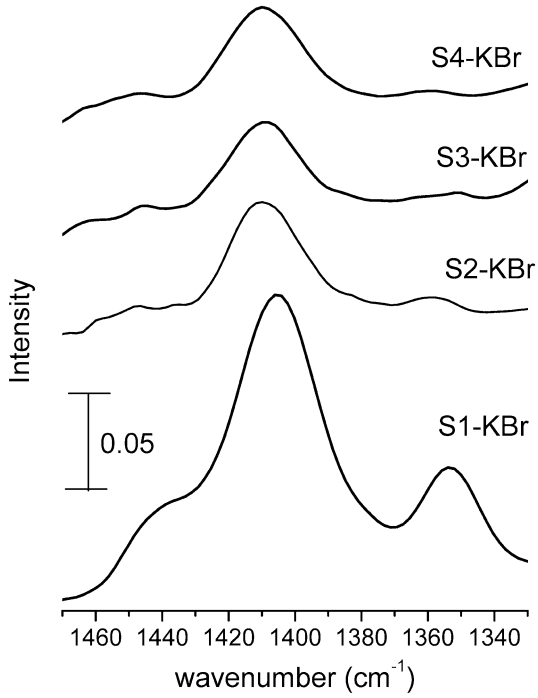

Figure 4. Magnification of the TO functions for samples S1−KBr to S4−KBr in the region of the wagging of CH_2 in $Si-CH_2-Si$ groups.

materials known as polycarbosilanes. In addition to this band, another important fingerprint of $Si-CH_2-Si$ groups is observed at ~1350 cm^{-1}.[7,34,42] Figure 4 shows an amplification of the TO function of the films in this region. It is a band assigned to the scissoring deformation (γ) of methylene groups,[34] which is not observed in the spectra of the samples deposited in the presence of O_2 (with the possible exception of sample S2−KBr, whose spectrum bears an extremely low-intensity band in this region). Because it is known that the ω_{CH2} band is much more intense than the γ_{CH2} band,[7,34,42] it can be supposed that $Si-CH_2-Si$ groups are important constituents of the skeleton of S1−KBr. In oxygen-free hexamethyldisilazane plasma polymers, both the ω_{CH2} and the γ_{CH2} in $Si-CH_2-Si$ groups were observed.[43−44] The issue of $Si-(CH_2)_n-Si$-group-containing silica structures (with $1 \leq n \leq 3$) have been recently investigated by Sugahara and co-workers.[45−47] For the film with $n = 1$, they did observe a band at ~1360 cm^{-1}, which was attributed to the γ_{CH2} in $Si-(CH_2)-Si$. It is important to stress that this band was not accompanied by the methylene C−H stretching bands. However, for films with $n = 2$, they have not observed the band at ~1360 cm^{-1} and started to observe both the C−H stretchings and two bands at 1280 and 1160 cm^{-1}, which, is related to $Si-CH_2CH_2-Si$.[32] Therefore, it seems that the presence of successive methylene groups plays an important role in the intensity and the position of CH_2-related bands.

From the spectrum of Figure 2, the formation of disilylethylene groups ($SiCH_2CH_2Si$) in film S1−KBr did not occur, because the spectrum did not show the characteristic in-phase wagging vibration of the two methylene groups, which lies between 1180 and 1120 cm^{-1}.[32] From all this discussion, it can be stated that the carbosilane groups present in our samples have $n = 1$.

It should be remembered that the AS1 mode of Si−O−Si groups could contribute to the 1030 cm^{-1} band in sample S1−KBr. The appearance of oxygen bonds in plasma-deposited films is not uncommon even when the monomer molecule does not contain oxygen and oxygen is not intentionally introduced into the discharge. Such oxygen contamination is assumed to originate from trace amounts of water vapor desorbed from the walls of the chamber during deposition, or from postdeposition reactions of free radicals in the film with oxygen and water vapor from the atmosphere.[3] Contamination by water can be clearly ruled out on examining the OH stretching region for the S1−KBr sample. However, the high-intensity associated with the Si−O−Si groups prevents us from discarding the possibility of a small oxygen contamination.

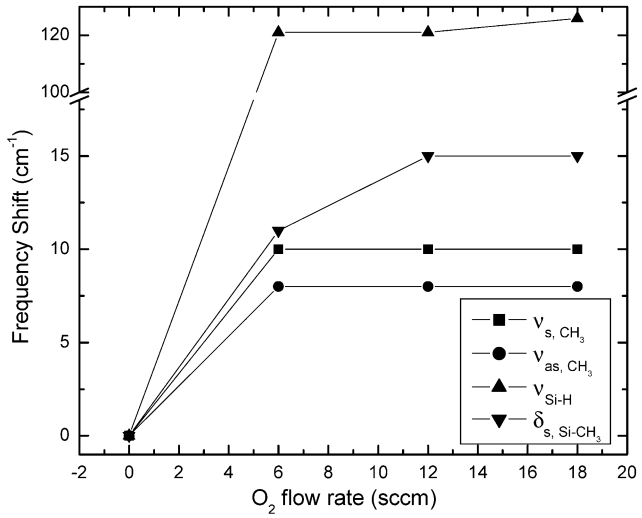

Figure 5. Frequency shifts of the $\nu_{S,CH3}$, $\nu_{AS,CH3}$, ν_{SiH}, and $\delta_{S,Si-CH3}$ modes as a function of the oxygen flow rate. The straight lines are a guide for the eye.

(4) Si−H and C═O. All of the films exhibited a band in the 2100−2250 cm^{-1} range that is attributable to Si−H stretching.[32] Their small intensities indicate that the quantity of Si−H bonds within the film is small. However, as discussed in the next section, such a band can be used as a probe of the overall incorporation of oxygen by the film.

The films deposited in the presence of O_2 presented small bands related to carbonyl species (~1620 and 1720 cm^{-1}),[40] which may be regarded as trace components of the films.

IVC. Oxygen Incorporation. The overall incorporation of oxygen atoms by the films can be evaluated through the peak positions of the C−H stretchings and CH_3 rockings in $Si-CH_3$ groups and the Si−H stretching. The Si−H stretching has proved to be sensitive both to local environment and to remote effects, i.e., to the electronegativity of the atoms bonded to the Si atom in the Si−H bond and to the overall "electronegativity" of the film. Extensive investigations on this matter have been carried out by Lucovsky and co-workers.[49−50] For our films, the frequency shift, $\Delta\nu$, of these bands was determined with respect to the same band in sample S1−KBr, as a function of the oxygen flow ratio in the gas feed. The results are represented in Figure 5.

It can be observed that the incorporation of oxygen in the films caused blue-shifts in the position of all of the bands that were analyzed. The blue-shift observed for the Si−H stretch is remarkable. The frequency of the band related to the stretching of Si−H groups in the film S1−KBr (2110 cm^{-1}) is higher than that observed for polymethylsilane [PMS, $(SiHCH_3)_x$, 2067 cm^{-1}][7] and this is significantly lower than that observed for polymethylsiloxane [PMSO, $(SiHCH_3O)_x$, 2160 cm^{-1}].[7] The latter is, in turn, inferior to those observed for films S2−KBr, S3−KBr, and S4−KBr (~2235 cm^{-1}). Because the position of this band is directly related to the electronegativity of the substituent atom bonded to the silicon, the shifts in its position are attributed to changes in the immediate neighborhood of the

silicon that bonds to the hydrogen: (Si)−Si−H in PMS, (CH_2)−Si−H in sample S1−KBr, and (O)−Si−H in PMSO. The fact that we have observed the Si−H stretching at frequencies higher than that observed for PMSO for the films deposited in the presence of O_2 suggests that they are highly oxidized. Investigating polymeric silsesquioxanes (structures whose skeleton is based on R−SiO_3 tetrahedra), Laine and co-workers[51] observed that when R was an H atom, the Si−H stretching was at ∼2250 cm^{-1}, which is not very far from the position we have observed in our films.

IVD. LO−TO Splittings. As described in section II, the LO−TO splitting is a phenomenon that has been observed both for crystalline and amorphous materials. In the area of amorphous materials, the LO−TO splitting of the AS1 mode in v-SiO_2 has been extensively documented.[8−19] However, as far as the authors are aware of, this is the first time that LO-TO splittings in organosilicon polymers have been reported.

First of all, it is important to note that only some bands in the spectra of all samples investigated presented an appreciable LO−TO splitting. In the high-frequency region, comprising the stretching of Si−H and C−H in methyl groups, the LO and TO functions nearly superpose each other. Such superposition may be due to a small oscillator strength,[52] which precludes LO−TO splittings, and/or to the fact that the oscillators are diluted within the solid so that they cannot undergo long-range Coulombic interactions and must be regarded as a local rather than a lattice vibration.

From the IR reflection−absorption studies of alkanethiol monolayers self-assembled on gold, carried out at very oblique incidence angles (e.g., 86°) and using p-polarized light (an excellent condition for the detection of LO modes), it is known that C−H stretchings do not undergo appreciable LO−TO splitting[53] as a consequence of their low oscillator strengths. Therefore, even if we had an extremely high density of C−H oscillators, the LO−TO splittings of stretching bands would not be appreciable. On the other hand, we have observed appreciable LO−TO splittings for the C−H bending and Si−C stretching modes. To analyze them, we will make the assumption that each LO−TO pair consists of nearest neighbors in the LO and TO functions, respectively. Although this is a sound assumption, we are aware of situations in which the rule can be broken, such as the AS2 mode in v-SiO_2.[9]

As shown in Figure 2, the only methyl bending band that does not give rise to an appreciable LO−TO splitting was the asymmetric methyl deformation (∼1410 cm^{-1}), which is very weakly IR active. On the other hand, the methyl symmetric deformation (∼1250 cm^{-1}) gives rise to a splitting of about 10 cm^{-1} for all samples. As a general trend, all of the LO−TO splittings for methyl bending modes increase as the oxygen concentration in the discharge decreases. For example, for the band related to methyl rocking and to the Si−C stretching in $SiMe_3$ groups, the LO−TO splitting ranges from 12 (for sample S4−KBr) to 24 cm^{-1} (for sample S1−KBr). This means that for these movements, the long-range Coulombic interactions were more efficient, and consequently, the density of methyl groups and/or Si−C bonds is higher, as the oxygen concentration decreased in the discharge. It can be argued that the dipole moment variation for that normal mode is dependent on the polar bond Si^+-C^-.

The frequencies of the TO and LO maxima and the LO-TO splittings for the AS1 mode of Si−O−Si groups are represented in Figure 6 as a function of the oxygen flow rate. As can be seen in the figure, the LO−TO splitting is relatively small when oxygen is not present in the gas feed but very large for the

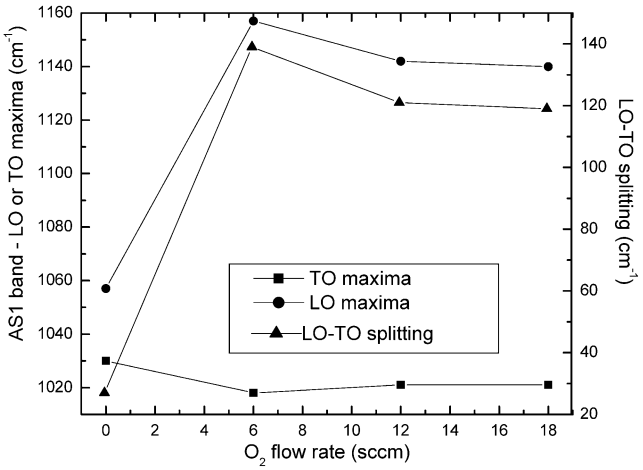

Figure 6. Maxima of the LO and TO functions and the LO-TO splitting of the AS1 mode as a function of the oxygen flow rate.

oxygen flow rates of 6.0, 12, and 18 sccm, reaching an apex for 6.0 sccm, corresponding to sample S2−KBr. This suggests that this is the film where there are more intense long-range Coulombic interactions and presupposes a higher density of Si−O−Si oscillators and a smaller quantity of defects, or discontinuities, that preclude long-range interactions. Assuming that the dipole moment for the AS1 mode has the same value for samples S2−KBr, S3−KBr, and S4−KBr, it can be estimated[52] that the concentration of Si−O−Si groups in sample S2−KBr is about 16% higher than in films S3−KBr and S4−KBr. Despite the low oxygen flow rate, this higher density in Si−O−Si oscillators in the S2−KBr film can be explained by the lower deposition rate (cf. Table 1). Smaller deposition rates in PECVD processes are often associated with more homogeneous films bearing fewer defects. The above discussion is a very important consequence of the assessment of F_{LO} because the small difference in the AS1-TO mode would not allow this inference.

The assessment of the LO functions for these organosilicon polymers has important implications on the spectral interpretation of reflection−absorption spectra taken at oblique incidence since they will preferentially detect LO modes.[54] Such a phenomenon is known as the Berreman Effect among spectroscopists and is relatively well documented in the literature. As discussed above, this phenomenon is not important for most organic compounds because, due to the low polar character of their bonds, long-range Coulombic coupling is not very effective. However, as exemplified in Figure 2, LO−TO splittings do occur for several characteristic vibrations of organosilicon species.

Figures 7 and 8 present both the experimental and simulated reflection−absorption spectra of samples S1−Al and S3−Al, respectively, taken at an incidence angle of 70° with p-polarized light in the 1600−400 cm^{-1} region. The simulated spectra are included to show that the line shape of the experimental spectrum is predicted by the Optical theory. The LO and TO functions, calculated from transmission measurements for samples S1−KBr and S3−KBr are also represented in Figures 7 and 8, respectively. A quick inspection of this figure is enough to notice that the absorption band maxima of the IRRAS spectra are closer to the maxima of the LO functions of these films than to the TO ones. Such phenomenon cannot be overlooked when one wants to assign IR bands of spectra taken in the reflection mode using literature data acquired at normal incidence in the transmission mode. Therefore, the importance of the Berreman Effect is 2-fold. On one hand, its experimental

TABLE 3: Possible Ending, Nonbranching, Branching, and Crosslinking Nodes Present in PECVD Films[a]

Ending Nodes	Non-Braching Nodes	Crosslinking and/or Branching Nodes	
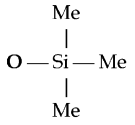	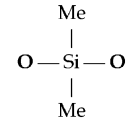	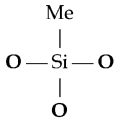	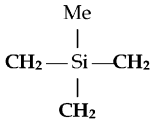
M	**D**	**T**	**$(CH_2)_3$**
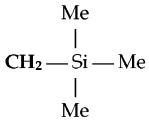	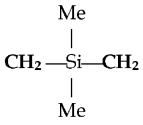	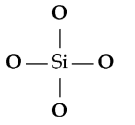	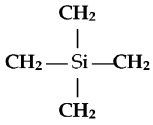
CH_2	**$(CH_2)_2$**	**Q**	**$(CH_2)_4$**

[a] Bridging groups are in bold letters (for simplification, the 0.5 underscore was omitted).

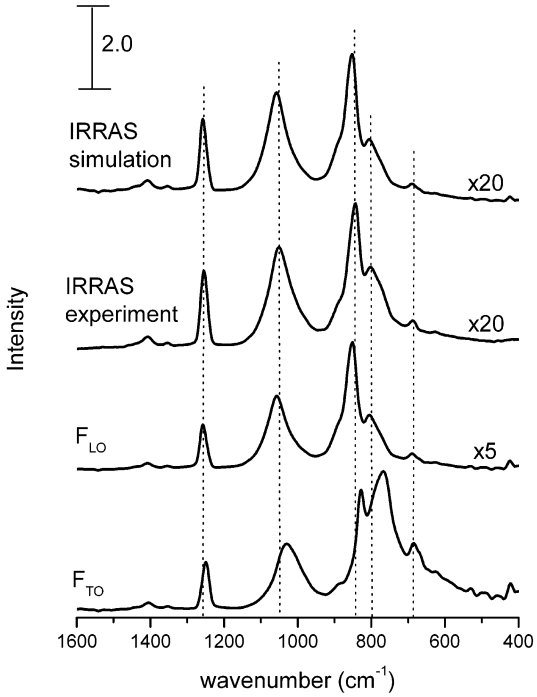

Figure 7. IRRAS spectrum of sample S1−Al and LO and TO functions calculated from the transmission spectrum of sample S1−KBr. The simulated IRRAS spectrum is also shown for comparison.

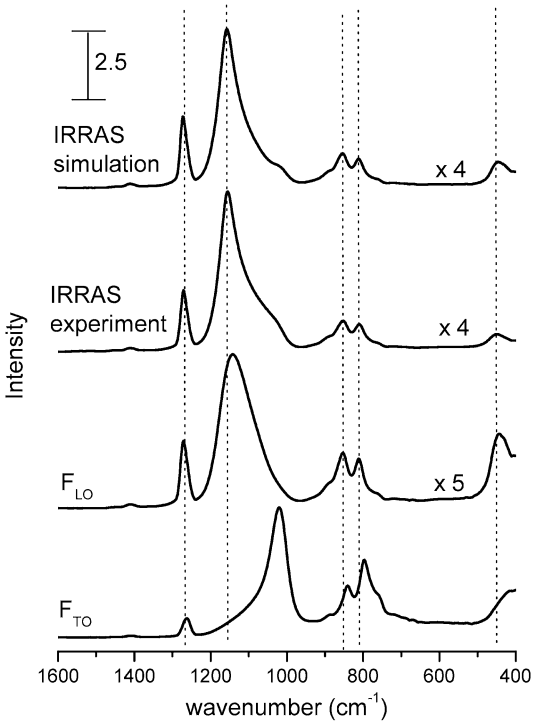

Figure 8. IRRAS spectrum of sample S3−Al and LO and TO functions calculated from the transmission spectrum of sample S3−KBr. The simulated IRRAS spectrum is also shown for comparison.

observation supports all of the discussion based on the dielectric functions determined through transmission measurements. On the other hand, it is fundamental to a correct interpretation of IRRAS spectra, as mentioned above.

IVE. Film Structure. Our discussion of the film structure will be made in terms of several basic chemical units in which a Si atom is bound to one or more oxygen atoms or methyl or methylene functional groups. These units are thus distorted tetrahedra centered on silicon atoms. They are represented in Table 3 and labeled according to a nomenclature analogous to that presented in ref 39. Here, M, D, T, and Q represent silicon atoms with increasing number of oxygen substituents and CH_2, $(CH_2)_2$, $(CH_2)_3$, and $(CH_2)_4$ represent nodes having methylene groups as bridging units. Note that Table 3 is not intended to be a rigorous summary of the silicon bonding environments present in our films, but it certainly describes the principal ones.

In general, the physical properties of all samples show evidence of intense cross-linking, because they are coherent, hard, and insoluble to common solvents such as propanol and acetone. First, let us focus on the samples deposited with oxygen in the gas feed. For these samples, the bridging unit between the distorted tetrahedra seems to be exclusively the oxygen atom. Only sample S2−KBr can have a trace amount of Si−CH_2−Si groups (Figure 4). It is also important to note that the Raman spectra of samples deposited in similar conditions did not show any bands attributable to Si−Si bonds.[45] The analysis of the methyl rocking and Si−C stretching bands shows the presence of M, D, and T nodes. However, the presence of Q nodes is also possible. Despite the concomitant presence of all these nodes, the AS1 band structure is relatively simple and consists of a single band with a high-frequency tail for the TO function.

This simplicity supports the idea of an overall random networked structure without domains where a specific type of node predominated. Otherwise, the different Si−O−Si group environments would give rise to band-broadening and even to clear-cut band splittings. At this point, it is interesting to compare our results to those obtained by Gleason and co-workers[39] for flexible films with a high polymeric character, for which the AS1 mode splits into two resolved bands similar to PMDS. The difference between the spectra of samples obtained in the batches S2, S3, and S4 to those of their films highlights the network character of our films.

Still considering only samples obtained with oxygen in the gas feed, the analysis of band maxima that are sensitive to oxygen incorporation by the films showed that, within the oxygen concentration range investigated, the amount of oxygen incorporated is only weakly affected by the amount of O_2 present in the discharge. An excessive amount of O_2 seems to promote extensive etching, as pointed out below, inducing the formation of more defective films.

An estimation based on the LO−TO splitting for the AS1 mode for samples S2−KBr, S3−KBr, and S4−KBr showed that the density increased as the oxygen flow rate decreased. Such densification is attributable to two factors: (i) to the decrease in the deposition rate and (ii) to the decrease of reactive oxygen species etching the solid film.

As for sample S1−KBr, methylene seems to be a bridging unit between the distorted tetrahedra. The IR characterization also identified $SiMe_x$ species, with x ranging from 1 to 3, which is coherent with a random network consisting of nodes such as CH_2, $(CH_2)_2$, and $(CH_2)_3$ (cf. Table 3). It is interesting to notice how intense is the depletion of methylene bridge incorporation through the addition of O_2 in the discharge. Such an observation seems to be connected to the decrease in carbon incorporation with the increase of oxygen in the discharge. Magni and co-workers[6] investigated plasmas of oxygen-diluted hexamethyldisiloxane (HMDSO) using mass spectrometry and IR spectroscopy. They found that hydrocarbon species detached from the monomer undergo oxidation, generating volatile compounds such as COH_2, CO_2H_2, CO, and CO_2. They have also observed that these species could be generated during film deposition through oxygen etching. Because methylene species are highly reactive toward oxygen, they react with oxygen as soon as they are formed, generating stable oxygenated organic gases. This results in a depletion of methylene incorporation by the material. Therefore, it seems that the main manner carbon is incorporated in the films deposited from oxygen-diluted plasmas is through methyl groups that remained bonded to monomeric fragments.

V. Conclusions

The present work reports, for the first time, the occurrence of LO−TO splittings of lattice vibrations in siloxane and carbosilane networks deposited by PECVD. A careful band assignment allowed the inference that the films deposited with oxygen in the gas feed were constituted of highly cross-linked methylsiloxane networks, whereas in those obtained in the absence of O_2, a network with a carbosilane skeleton was synthesized. It is interesting to stress the fact that the presence of O_2 in the discharge completely precluded the formation of CH_2 bridges, inducing the enrichment of the material in Si−O−Si groups. Although the amount of methyl groups increased with the decrease of O_2 flow rate, the analysis of the LO−TO frequencies permitted inferring that the concentration of Si−O−Si oscillators was greater for the solid synthesized with the highest Ar-to-O_2 flow ratio. This is in accordance with previously reported studies showing that an excess of O_2 could attack the film and increase the amount of defects, such as dangling bonds, chain termination, and porosity. Finally, the assessment of LO and TO functions was important for the interpretation of reflection−absorption spectra of films deposited onto aluminum.

Acknowledgment. The Fundação de Amparo à Pesquisa do Estado de São Paulo, FAPESP, is acknowledged for financial support (Grant Nos. 98/11743-2, 98/10979-2, and 02/07482-6) as is the Conselho Nacional de Desenvolvimento Científico e Tecnológico, CNPq. We are also indebted to Dr. Donald C. McKean for enlightening discussions about band assignments, to Dr. M. Isabel Felisberti for clarifying discussions regarding polymer terminology, to Mr. Donga de Souza and Dr. Lucila Cescato for their assistance in the index of refraction measurements, and to Dr. Carol H. Collins and Dr. Steve F. Durrant for revising this manuscript.

References and Notes

(1) Pai, P. G.; Chao, S. S.; Takagi, Y.; Lukovsky, G. *J. Vac. Sci. Technol. A* **1986**, *4*, 689.
(2) Furusawa, T.; Daisuke, R.; Yoneyama, R.; Homma, Y.; Hinode, K. *Electrochem. Solid-State Lett.* **2001**, *4*, G31.
(3) Da Cruz, N. C.; Durrant, S. F.; Bica de Moraes, M. A. *J. Polym. Sci.: Part B: Polym Phys.* **1998**, *36*, 1873.
(4) Hinds, B. J.; Wang, F.; Wolfe, D. M.; Hinkle, C. L.; Lucovsky, G. *J. Non-Cryst. Solids* **1998**, *227*, 507.
(5) Wolfe, D. M.; Hinds, B. J.; Wang, F.; Lucovsky, G.; Ward, B. L.; Xu, M.; Nemanich, R. J. *J. Vac. Sci. Technol. A* **1999**, *17*, 2170.
(6) Magni, D.; Descheneaux, C.; Hollenstein, C.; Creatore, A.; Fayet, P. *J. Phys. D: Appl. Phys.* **2001**, *34*, 87.
(7) Scarlete, M.; Brienne, S.; Butler, I. S.; Harrod, J. F. *Chem. Mater.* **1994**, *6*, 977.
(8) Harbecke, B.; Heinz, B.; Grosse, P. *Appl. Phys. A* **1985**, *38*, 263.
(9) Kirk, C. T. *Phys. Rev. B* **1988**, *38*, 1255.
(10) Almeida, R. M. *Phys. Rev. B* **1992**, *45*, 161.
(11) Kamitsos, E. I.; Patsis, A. P.; Kordas, G. *Phys. Rev. B* **1993**, *48*, 12499.
(12) Guiton, T. A.; Pantano, C. G. *Colloids Surf. A: Physicochem. Eng. Aspects* **1993**, *74*, 33.
(13) Almeida, R. M. *Phys. Rev. B* **1996**, *53*, 14656.
(14) Kamitsos, E. I. *Phys. Rev. B* **1996**, *53*, 14659.
(15) Sarnthein, J.; Pasquarello, A.; Car, R. *Science* **1997**, *275*, 1925.
(16) Pasquarello, A.; Car, R. *Phys. Rev. Lett.* **1997**, *79*, 1766.
(17) Martinet, C.; Devine, R. A. B. *J. Appl. Phys.* **1997**, *81*, 6996.
(18) Queeney, K. T.; Weldon, M. K.; Chang, J. P.; Chabal, Y. J.; Gurevich, A. B.; Sapjeta, J.; Opila, R. L. *J. Appl. Phys.* **2000**, *87*, 1322.
(19) Trasferetti, B. C.; Davanzo, C. U. *Appl. Spectrosc.* **2000**, *54*, 502.
(20) Kittel, C. *Introduction to Solid State Physics*, 7th ed.; John Wiley & Sons: New York, 1996.
(21) Blakemore, J. S. *Solid State Physics*, 2nd ed.; Cambridge Universtiy Press: Cambridge, 1995.
(22) Galeener, F. L.; Lucovsky, G. *Phys Rev. Lett.* **1976**, *37*, 1474.
(23) Sekimoto, K.; Matsubara, T. *Phys. Rev. B* **1982**, *26*, 3411.
(24) Payne, M. C.; Inkson, J. C. *J. Non-Cryst. Solids* **1984**, *68*, 351.
(25) de Leeuw, S. W.; Thorpe, M. F. *Phys. Rev. Lett.* **1985**, *55*, 2879.
(26) Devine, R. A. B. *Appl. Phys. Lett.* **1996**, *68*, 3108.
(27) The refractive index was measured by the Abelès method. In brief, it consists of measuring the incident angle for which the film reflection vanishes. The method was performed by using an expanded, collimated and p-polarized He−Ne laser ($\lambda = 633$ nm). The reflected light spot is observed on a screen by rotating the goniometer with the sample, until the step formed from the film to the substrate remains the same. The angles in which the intensity reflected from both film and substrate are the same correspond to the "Brewster angle" whose tangent is the refractive index of the film. For another example of this procedure, see: de Souza, D. R.; Soares, L. L.; Cescato, L.; Alves, M. A. R.; Braga, E. S. *Microelectron. J.* **2000**, *31*, 251.
(28) Yamamoto, K.; Ishida, H. *Vib. Spectrosc.* **1994**, *8*, 1.
(29) Hawranek, J. P.; Jones, R. N. *Spectrochim. Acta* **1976**, *32*, 99.
(30) Ten, Y.-S.; Wong, J. S. *J. Phys. Chem.* **1989**, *93*, 7208.
(31) Smith, D. Y.; Shiles, E.; Inokuti, M. In *Handbook of Optical Constants of Solids*; Palik, E. D., Ed., Academic Press: Orlando, 1985.
(32) Anderson, D. R. In *Analysis of silicones*; Smith, A. L., Ed.; John Wiley & Sons: New York, 1974.

(33) Marchand, A.; Valade, J.; Forel, M.-T.; Josien, M.-L.; Calas, R. J. *Chim. Phys.* **1962**, *59*, 1142.
(34) McKean, D. C.; Davidson, G.; Woodward, L. A. *Spectrochim. Acta A* **1970**, *26*, 1815.
(35) Lee Smith, A.; Anderson, D. R. *Appl. Spectrosc.* **1984**, *38*, 822.
(36) McKean, D. C. *Spectrochim. Acta A* **1999**, *55*, 1485.
(37) Fleischer, H.; McKean, D. C. *J. Phys. Chem. A* **1999**, *103*, 727.
(38) Bellamy, L. J. *The Infra-Red Spectra of Complex Molecules*; Chapman & Hall: London, 1975
(39) Pryce Lewis, H. G.; Edell, D. J.; Gleason, K. K. *Chem. Mater.* **2000**, *12*, 3488.
(40) Tsu, D. V.; Lucovsky, G.; Davidson, B. N. *Phys. Rev. B* **1989**, *40*, 1795.
(41) Pryce Lewis, H. G.; Casserly, T. B.; Gleason, K. K. *J. Electrochem. Soc.* **2001**, *148*, F212.
(42) Rau, C.; Kulisch, W. *Thin Solid Films* **1994**, *249*, 28.
(43) Wróbel, A. M.; Wertheimer, M. R.; Dib, J.; Schreiber, H. P. *J. Macromol. Sci.—Chem.* **1980**, *A14*, 321.
(44) Wróbel, A. M.; Kryszewski, M.; Gazicki, M. *J. Macromol. Sci.—Chem.* **1983**, *A20*, 583.
(45) Sugahara, S.; Usami, K.; Matsumura, M. *Jpn. J. Appl. Phys.* **1999**, *38*, 1428.
(46) Sugahara, S.; Kadoya, T.; Usami, K.; Hattori, T.; Matsumura, M. *J. Electrochem. Soc.* **2001**, *148*, F120.
(47) Usami, K.; Sugahara, S.; Kadoya, T.; Matsumura, M.; Proc. 7th International Sumposium on Quantum Effect Electronics; Tokyo Institute of Technology; 2000 (http://www.pe.titech.ac.jp/qee_root/symposium/symposium2000program.htm).
(48) Trasferetti, B. C.; Davanzo, C. U.; de Moraes, M. A. B. unpublished results.
(49) Lucovsky, G. *J. Non-Cryst. Solids* **1998**, *227*, 1.
(50) Lucovsky, G. *Solar Cells* **1980**, *2*, 431.
(51) Zhang, C.; Barbonneau, F.; Bonhomme, C.; Laine, R. M.; Soles, C. L.; Hristov, H. A.; Yee, A. F. *J. Am. Chem. Soc.* **1998**, *120*, 8380.
(52) LO−TO splittings are related to the dipole moment derivative through the following equation: $\nu_{LO}^2 - \nu_{TO}^2 = (N/\pi c^2)[(n_\infty + 2)/3n_\infty]^2 (\partial\mu/\partial q)^2$. In this expression, n_∞ is the refractive index at high frequency, N is the number of molecules/cm^3 and $\partial\mu/\partial$q is the derivative of the dipole moment with respect to the normal coordinate for ν_0 (0→1), which is the frequency of the oscillator "expected in the absence of the long-range, electrostatic coupling" [See: Decius, J. C. *J. Chem. Phys.* **1968**, *49*, 1387 and Jones, L. H.; Swanson, B. I. *J. Phys. Chem.* **1991**, *95*, 2701]. If we assume that $\partial\mu/\partial$q for the AS1 mode is the same for samples S2, S3, and S4, we can estimate the ratios between the parameter N for any pair of samples.
(53) Allara, D. L.; Nuzzo, R. G. *Langmuir* **1985**, *1*, 52.
(54) Berreman, D. W. *Phys. Rev.* **1963**, *130*, 2193.